Mechanisms for Lithium Insertion in Carbonaceous Materials

J. R. Dahn,* Tao Zheng, Yinghu Liu, J. S. Xue

Lithium can be inserted reversibly within most carbonaceous materials. The physical mechanism for this insertion depends on the carbon type. Lithium intercalates in layered carbons such as graphite, and it adsorbs on the surfaces of single carbon layers in nongraphitizable hard carbons. Lithium also appears to reversibly bind near hydrogen atoms in carbonaceous materials containing substantial hydrogen, which are made by heating organic precursors to temperatures near 700°C. Each of these three classes of materials appears suitable for use in advanced lithium batteries.

There are hundreds of commercially available carbon types, including natural and synthetic graphites, carbon blacks, active carbons, carbon fibers, cokes, and a wide variety of other materials prepared by the pyrolysis of organic precursors in inert gas. All of these materials reversibly react with lithium to some extent and can be used as the negative electrode in lithium-ion batteries (*1*). To maximize the stored energy per unit mass in these batteries, it is crucial to determine which types of carbon react reversibly with the largest amount of lithium per unit mass of carbon. Hundreds of carbon types have been tested for this application (*2*) and three classes of commercially relevant lithium-battery carbons have emerged.

Carbon Types

Figure 1 shows the maximum amount of lithium with which carbons can reversibly react as a function of the heat treatment temperature for carbons prepared by the pyrolysis of organic precursors. These data were collected by electrochemically reacting lithium with the carbons in cells with lithium metal as one electrode and with a particular carbon sample as the other electrode. In such an experiment, the Li atoms are transferred from the metal to the carbon as ions (through the cell electrolyte) and electrons (through the external circuit). Battery scientists measure the number of electrons transferred through the external circuit per gram of carbon; this quantity is the specific capacity of the carbon in milliampere-hours per gram. Because one lithium ion is transferred for each electron, the specific capacity can be related to the stoichiometry of the carbon electrode. For example, if one Li atom is transferred per six C atoms [the maximum limit for graphite under ambient conditions (*2*)], a specific capacity of 372 mA·hour g^{-1} results.

Most striking about Fig. 1 is the large variation in specific capacity that occurs as a function of heat treatment temperature and carbon type. To understand this variation we must consider the structure and chemistry of carbons prepared by the heating of organic precursors. Fortunately, this is a well-studied field (*3*). During the early stages of pyrolysis in inert gas (below 600°C), organic compounds decompose and emit gases that contain carbon, such as CO and CH_4 (*4*). The remaining C atoms condense into planar aromatic structures (called graphene sheets) that are terminated predominantly with H atoms at their edges. If the decomposing precursor forms a semifluid state, then these planar sheets can align in a more or less parallel fashion that leads ultimately to easy graphitization upon heating to very high temperatures. Such precursors yield "soft" or graphitizable carbons. However, if the organic precursor is sufficiently cross-linked, then a fluid state is not realized during decomposition and the planar aromatic structures cannot align. These materials are difficult to graphitize at any heat treatment temperature and thus are called "hard" or nongraphitizable carbons.

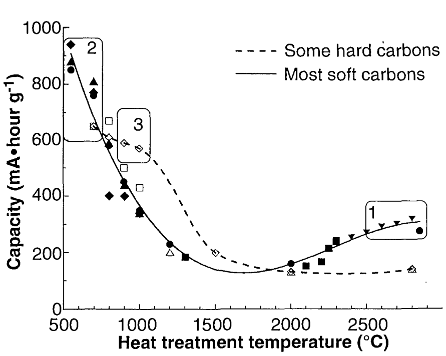

Fig. 1. Plot of reversible capacity for lithium versus heat treatment temperature for a variety of carbon samples (open symbols, hard carbons; solid symbols, soft carbons). These data are for the second charge-discharge cycle of lithium-carbon test cells. The three regions of commercial relevance are shown.

During heating in the temperature range from 600° to ~1000°C, hydrogen is eliminated (*4*) and the size of the planar graphene sheets grows to ~20 to 30 Å. In soft carbons, there are regions where 3 to 10 of these sheets are stacked in a more or less parallel fashion, separated by small regions of "unorganized carbon" that may consist of buckled single layers or tetrahedrally bonded carbon (*5*). The layers are stacked with random rotations or translations between them, a condition known as turbostratic disorder (*6*). In some hard carbons, the graphene sheets do not stack in a parallel way and are in a "house of cards" arrangement. Such carbons inherently have appreciable nanoporosity, with pores on the order of the size of the graphene sheets (*7*).

During further heating of soft carbons above 1000°C, the lateral dimensions of the graphene sheets grow to ~150 Å; by 2000°C, the layers become parallel (with 50 to 100 layers per stack) but turbostratic misalignment is not relieved, apparently because of some "pinning" that prevents the rotation of layers into the normal stacking found in graphite. Only above 2000°C is enough thermal energy present to overcome this pinning and for the layers to rotate into the registered graphite stacking arrangement. The probability *P* of finding adjacent graphene sheets in turbostratic misalignment decreases from ~1 at 2000°C to near 0 for soft carbons heated to ~3000°C. As hard carbons are heated above 1000°C, the size of the graphene sheets grows and the sheets swing into more or less parallel positions, eliminating the nanoporosity. However, large numbers of parallel layers never form at any heat treatment temperature and turbostratic misalignment is never relieved.

Carbons in the three highlighted regions of Fig. 1 are currently used or have been proposed for use in commercial lithium-ion batteries. Region 1 contains carbons prepared by heating so-called soft carbon precursors to temperatures above ~2400°C, where well-graphitized materials result. In these materials, the probability *P* for turbostratic misalignment between adjacent layers decreases with heating temperature. Region 2 contains both soft and hard carbon precursors that contain substantial hydrogen. As the temperature of the samples is

---

The authors are in the Department of Physics, Simon Fraser University, Burnaby, British Columbia V5A 1S6, Canada.

*To whom correspondence should be addressed.

increased, the hydrogen content decreases. Region 3 contains hard carbon materials that are made up predominantly of single carbon sheets that contain appreciable nanoporosity and are stacked more or less like a house of cards. All of the data in Fig. 1 were collected in our laboratory. Carbons in regions 1, 2, and 3 have been discussed in (*8–10*), respectively, where we proposed mechanisms for the variation of specific capacity with heating temperature in each region.

Figure 2 shows the voltage-capacity relations for lithium-carbon electrochemical cells made from representative materials from each of the three regions of Fig. 1. The synthetic graphite sample gives a reversible capacity of ~355 mA·hour g^{-1}. Petroleum pitch heated to 550°C to give $H_{0.4}C$ (*9*) gives a reversible capacity of near 900 mA·hour g^{-1}, one of the largest capacities of any material in region 2. All materials in region 2 are anomalous because their voltage profiles show appreciable hysteresis (lithium inserted near 0.0 V is removed near 1 V). Resole resin heated to 1000°C has a composition of $H_{0.04}C$ and gives a reversible capacity of ~560 mA·hour g^{-1}, one of the largest capacities known for materials in region 3. The voltage profiles for each of the materials in Fig. 2 are markedly different, which suggests that different reaction mechanisms are important in each of the three regions in Fig. 1.

Graphitic Carbons—Region 1

Graphite can intercalate up to one Li atom per six C atoms under ambient conditions (*11*). In LiC_6, the Li atoms occupy next nearest-neighbor sites, separated by 4.25 Å, within the van der Waals space between every pair of carbon sheets (*12*). When the lithium is intercalated, it transfers most of its 2*s* electron density to the carbon host and exists as a screened ion between the carbon sheets. The Coulomb repulsion between lithium ions in nearest-neighbor sites is apparently greater than the binding energy of the lithium to the graphite host, so that mixtures of metallic lithium and Li_xC_6 coexist when samples of composition $x > 1$ in Li_xC_6 are attempted at room temperature and pressure.

Recently, Nalimova *et al.* (*13*) showed that samples of $x > 1$ could be prepared in graphite under the extreme conditions of 280°C and 50 kbar on molten lithium in contact with the graphite. Apparently, these conditions are sufficient to induce the occupation of nearest-neighbor sites in Li_xC_6. However, we do not believe that nearest-neighbor sites are occupied in any of the carbons in regions 1, 2, and 3 under ambient conditions for the following reason: Lithium intercalates into solids because its chemical potential is lowered relative to that in elemental lithium. The change in chemical potential includes a $P\Delta V$ term, which can be estimated. If we assume that the molar volume of lithium metal or liquid is 14 cc mol^{-1} and that 6 mol of graphite expands by 10% upon intercalation of 1 mol of lithium, then $\Delta V \approx -11$ cc per mole of intercalated Li and $P\Delta V/P \approx 10^{-5}$ eV $atom^{-1}$ bar^{-1}. At ambient pressure, this contribution to the chemical potential change is negligible, but at 50 kbar, $P\Delta V \approx -0.5$ eV $atom^{-1}$. Therefore, at 50 kbar, we are effectively able to access voltages down to ~ -0.5 V versus Li at ambient pressure. If the insertion of lithium into nearest-neighbor sites requires 50 kbar, then it effectively occurs near −0.5 V in Fig. 2. In the experiments of Fig. 2, such voltages can not be reached, because metallic Li electrodeposits on the carbon surface at all voltages below 0 V in equilibrium. Thus, it is unlikely that near-neighbor sites can be filled by lithium in carbonaceous materials under ambient conditions.

When lithium intercalates between adjacent parallel carbon sheets, these sheets rotate from "AB" registry (*14*) into "AA" registry (*15*), with honeycombs directly above and below one another. The Li atoms are centered between honeycombs above and below; therefore, lithium might not intercalate between adjacent layers that are turbostratically misaligned and pinned. Figure 3 (*8*) is a plot of the reversible capacity of region 1 carbons (heated above 2200°C) versus *P*, the probability of turbostratic misalignment in adjacent parallel layers. The capacity *Q* varies as $Q = 372(1 - P)$, as expected on the basis of the arguments above; this finding suggests that no lithium can be inserted between adjacent parallel layers that are turbostratically misaligned.

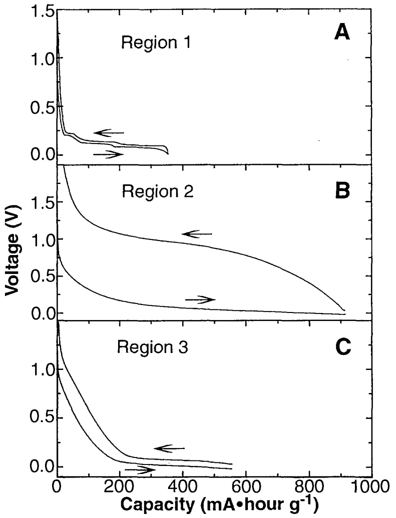

Fig. 2. Plots of voltage versus reversible capacity for the second charge-discharge cycle of representative carbon samples from regions 1, 2, and 3 of Fig. 1. (**A**) Synthetic graphite (Johnson-Matthey); (**B**) petroleum pitch (Crowley Tar Co.) heated to 550°C; (**C**) resole resin (Occidental Chemical Co.) heated to 1000°C. Arrows designate the directions the curves are traversed as Li is added to (to the right) or removed from (to the left) the carbon samples.

Hydrogen-Containing Carbons—Region 2

A variety of materials pyrolyzed at temperatures near 700°C show behavior similar to that in Fig. 2B (*16–18*). Mabuchi *et al.* (*16*) argued that large amounts of lithium are being inserted within "cavities" in these materials. However, our recent work (*10*) shows that these materials offer little evidence for microporosity. Moreover, such an explanation would require the chemical potential of the inserted lithium to be very close to that of metallic lithium, because it would only be weakly bound to the carbon; in experiments like those of Fig. 2B, a cell voltage of several tens of millivolts would be expected, and no hysteresis would be expected. Sato *et al.* (*17*) proposed that the Li atoms intercalate and occupy nearest-neighbor sites between each pair of graphene sheets. This explanation would require some mechanism for the lithium ions to overcome the large screened Coulomb repulsion between ions on nearest-neighbor sites in the absence of a huge applied pressure on the lithium. Sato's mechanism invokes the equilibrium occupation of these sites, so this explanation would not be expected to lead to hysteresis in the voltage profile.

Yata *et al.* (*18*) realized that carbons prepared at these temperatures contain substantial hydrogen and therefore called the materials they prepared from pyrolyzed phenolic resins "polyacenic semiconductors." Typically, the materials that showed high capacity for lithium in (*16–18*) had H/C

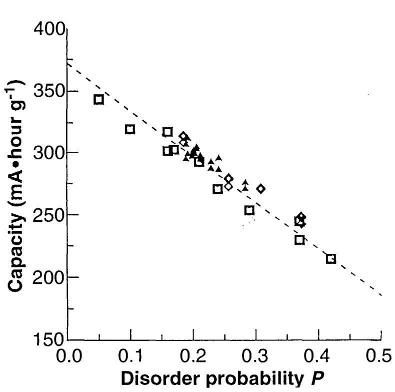

Fig. 3. Reversible capacity of region 1 carbons plotted as a function of the probability *P* of turbostratic disorder between adjacent carbon sheets. The line is the relation $Q = 372(1 - P)$, where *Q* is the capacity. For the purposes of this plot, samples corresponding to different symbols are equivalent.

atomic ratios in the neighborhood of 0.2. Because the hydrogen in these materials could be playing a crucial role in the mechanism of lithium insertion, we synthesized a series of materials at different temperatures from petroleum pitches, polyvinyl chloride, and polyvinylidene fluoride. Figure 4 shows the correlation between reversible specific capacity and H/C atomic ratio for these region 2 materials (*9*). The solid line in Fig. 4 is that expected if each H atom can bind to a Li atom within the solid and if a hydrogen-free soft carbon heated to near 1000°C has a capacity of 300 mA·hour g^{-1}. Even the data from (*16*) fit nicely in the trend. Note that the data in Fig. 4 are for the second charge-discharge cycle of these cells; these materials do not maintain their large capacities for more than a dozen or so cycles (*9*).

The substantial work that has been done on ternary graphite-alkali-hydrogen materials may be important to our observations in Fig. 4. In a massive review of the subject (*19*), Enoki *et al.* showed that charge transfer from alkalis to hydrogen in carbons is expected. Therefore, we believe that Li atoms can bind in the vicinity of H atoms in these hydrogen-containing carbons. The inserted lithium could transfer part of its 2*s* electron (in a covalent bond) to a nearby hydrogen, resulting in a corresponding change to the H–C bond. This would cause changes in the relative atomic positions of the C and H atoms; these bonding changes would be activated processes, which can lead to hysteresis. Bonding changes in the host have been shown to cause hysteresis in such electrochemical measurements (*20*). During charging, when the lithium is removed from the carbon, the original H–C bonds would reform. If the reforming of the bonds is not complete, then it is likely that the cycling capacity would slowly decay, as observed (*9*). We stress that we do not believe that bulk lithium hydride is being formed in these materials, and further work is needed to determine exactly how the lithium is attached near the hydrogen.

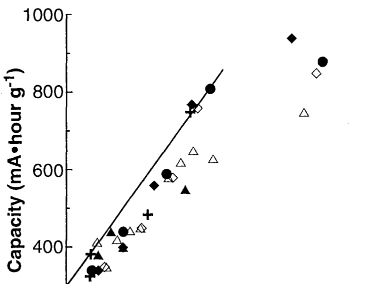

Fig. 4. Reversible capacity of region 2 carbons plotted as a function of their hydrogen content. Samples [●, Crowley pitch; ◇, KS pitch series A (Kureha Co., Japan); △, KS pitch series B (Kureha); ◆, polyvinyl chloride; ▲, polyvinylidene fluoride] were heated to temperatures between 550° and 1000°C. Data from (*16*) are also shown (+). The solid line assumes that each H atom can reversibly bind with one Li atom.

Hard Carbon Precursors—Region 3

A number of carbons with voltage profiles similar to that in Fig. 2C have been reported. Materials that show a low voltage plateau with a capacity of several hundred milliampere-hours per gram and little hysteresis have been prepared by Omaru *et al.* (*21*) from pyrolyzed polyfurfuryl alcohol, by Takahashi *et al.* (*22*) from unspecified precursors, by Sonobe *et al.* (*23*) from pyrolyzed petroleum pitch, and by Liu *et al.* (*10*) from pyrolyzed epoxy novolac resin. Ishikawa *et al.* (*24*) believe that such a capacity corresponds to the filling of micropores in the carbon by clusters of lithium. This mechanism would be expected to give weakly bound lithium (relative to that in Li metal) and hence a very low voltage plateau, consistent with experimental results (Fig. 2C).

In our earlier work (*10*), we showed that these carbon materials consisted primarily of small single layers of carbon arranged more or less like a house of cards. We proposed that lithium could be adsorbed on both of the surfaces of these single sheets, leading to more lithium per carbon than in intercalated graphite. In lithium-intercalated graphite, there is one layer of intercalated lithium for each carbon sheet. In carbons composed mainly of single layers, Li atoms at the same areal density presumably could be adsorbed on each side of the sheet, leading to two layers of lithium for each carbon sheet and hence a theoretical maximum capacity of Li_2C_6 or 740 mA·hour g^{-1}. To test this hypothesis, we prepared a series of carbons with varying fractions of single layers (*10*) and measured how much lithium could be inserted within them. Figure 5 shows that the reversible specific capacity of these region 3 materials increases with their single-layer fraction. Small-angle x-ray scattering (SAX) showed that each of the materials with a capacity of >400 mA·hour g^{-1} in Fig. 5 contained appreciable nanoporosity (*10*).

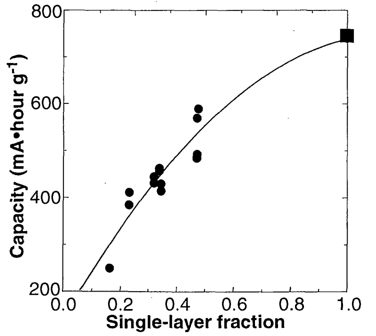

Fig. 5. Reversible capacity of region 3 carbons prepared from epoxy-novolac resins heated between 900° and 1100°C plotted as a function of their single-layer fraction. The square point is that hypothesized for complete adsorption on both sides of a carbon consisting only of single layers, and the line is a guide for the eye.

It is easy to reconcile the surface adsorption model proposed here with the pore-filling model of Ishikawa *et al.* (*24*). When the pores become small enough (SAX shows that they are on the order of 15 Å in diameter), the adsorption of lithium on the pore surfaces will essentially fill the pores entirely. In both models, we expect the lithium to be weakly bound (relative to that in Li metal), consistent with the low voltage plateau in Fig. 2C. In the sample used in Fig. 2C, ∼50% of the C atoms were in single layers, with the remainder in double- and triple-layer groupings. The steeply sloping portion of the voltage profile in Fig. 2C is thought to arise from the insertion of lithium between carbon layers that are stacked in a roughly parallel fashion.

Conclusions

Three different mechanisms appear to be responsible for the insertion of lithium in carbonaceous materials that are relevant to the battery industry. In graphitic carbons (region 1), intercalation occurs, but lithium cannot be accommodated between adjacent carbon layers that show turbostratic disorder. In carbons that contain substantial amounts of hydrogen (region 2), the maximum amount of lithium that can be inserted is proportional to the hydrogen content, which suggests that the lithium binds somehow in the vicinity of the H atoms. The voltage-capacity behavior of the hydrogen-containing carbons shows large hysteresis. In materials that are made up predominantly of single layers of carbon and hence inherently incorporate nanopores (region 3), lithium appears to adsorb on both sides of the carbon layers. The work presented here and in (*8–10*) qualitatively identifies the dominant physical mechanisms for the reaction of lithium with the important carbon types. Substantial experimental and theoretical work is needed before these mechanisms can be considered proven.

REFERENCES AND NOTES

1. For some recent reviews on lithium-ion batteries, see G. Stix, *Sci. Am.* 108 (October 1993); G. Pistoia, Ed., *Lithium Batteries, New Materials and New Perspectives* (Elsevier North-Holland, New York, 1993); or the special issue on Lithium Batteries, J. M. Tarascon, Ed., *Solid State Ionics* **69** (1994), which contains numerous useful articles (in particular, K. Brandt, p. 173).
2. Some recent reviews include J. R. Dahn *et al., Electrochim. Acta* **38**, 1179 (1993); J. R. Dahn *et al.*, in *Lithium Batteries, New Materials and New Perspec-*

tives, G. Pistoia, Ed. (Elsevier North-Holland, New York, 1993), pp. 1–47.
3. Numerous reviews on this topic can be found in the series *Chemistry and Physics of Carbon,* P. L. Walker Jr., Ed. (Dekker, New York), vol. 1-26.
4. K. Ouchi and H. Honda, *Fuel* **38**, 429 (1959).
5. R. E. Franklin, *Proc. R. Soc. London Ser. A* **209**, 196 (1951).
6. B. E. Warren, *Phys. Rev.* **59**, 693 (1941).
7. See, for example, A. Gupta and I. R. Harrison, *Carbon* **32**, 953 (1994).
8. T. Zheng, J. N. Reimers, J. R. Dahn, *Phys. Rev. B* **51**, 734 (1995).
9. T. Zheng *et al., J. Electrochem. Soc.* **142**, 2581 (1995).
10. Y. Liu, J. S. Xue, T. Zheng, J. R. Dahn, *Carbon,* in press.
11. J. E. Fischer, in *Chemical Physics of Intercalation,* A. P. Legrand and S. Flandrois, Eds. (Plenum, New York, 1987), pp. 59–78.
12. N. Kambe *et al., Mater. Sci. Eng.* **40**, 1 (1979).
13. V. A. Nalimova, D. Guerard, M. Lelaurain, O. Fateev, *Carbon,* in press.
14. W. A. Harrison, *Electronic Structure and the Properties of Solids* (Dover, New York, 1989).
15. R. C. Boehm and A. Bannerjee, *J. Chem. Phys.* **96**, 1150 (1992).
16. A. Mabuchi, K. Tokumitsu, H. Fujimoto, T. Kasuh, 7th International Meeting on Lithium Batteries, Boston, 15–20 May, 1994 (extended abstracts, paper I-A-10), p. 207.
17. K. Sato, M. Noguchi, A. Demachi, N. Oki, M. Endo, *Science* **264**, 556 (1994).
18. S. Yata *et al., Synth. Met.* **62**, 153 (1994).
19. T. Enoki, S. Miyajima, M. Sano, H. Inokuchi, *J. Mater. Res.* **5**, 435 (1990).
20. For example, hysteresis in Li electrochemical cells was observed when Mo–S bonds in $LiMoS_2$ were broken as the result of the formation of Li-S bonds upon further insertion of lithium [see L. S. Selwyn, W. R. McKinnon, U. von Sacken, C. A. Jones, *Solid State Ionics* **22**, 337 (1987)].
21. A. Omaru, H. Azuma, M. Aoki, A. Kita, Y. Nishi, 182nd Meeting of the Electrochemical Society, Toronto, Canada, 12–16 October 1992 (extended abstracts of Battery Division, paper 25), p. 34.
22. Y. Takahashi *et al.,* 35th Battery Symposium in Japan, Nagoya, 14–16 November 1994 (extended abstracts), p. 39.
23. N. Sonobe, M. Ishikawa, T. Iwasaki, *ibid.,* p. 47.
24. M. Ishikawa, N. Sonobe, H. Chuman, T. Iwasaki, *ibid.*, p. 49.

Neurotrophins and Neuronal Plasticity

Hans Thoenen

There is increasing evidence that neurotrophins (NTs) are involved in processes of neuronal plasticity besides their well-established actions in regulating the survival, differentiation, and maintenance of functions of specific populations of neurons. Nerve growth factor, brain-derived neurotrophic factor, NT-4/5, and corresponding antibodies dramatically modify the development of the visual cortex. Although the neuronal elements involved have not yet been identified, complementary studies of other systems have demonstrated that NT synthesis is rapidly regulated by neuronal activity and that NTs are released in an activity-dependent manner from neuronal dendrites. These data, together with the observation that NTs enhance transmitter release from neurons that express the corresponding signal-transducing Trk receptors, suggest a role for NTs as selective retrograde messengers that regulate synaptic efficacy.

Neurotrophic factors have been considered predominantly with respect to their functions in regulating the survival and differentiation of selective populations of neurons during embryonic development and the maintenance of specific functions of those neurons in adulthood (*1*). The spectrum of the biological actions of neurotrophins (NTs) [the general term coined for members of the nerve growth factor (NGF) gene family] is determined by the site and extent of their expression (*2*) and of the expression of the corresponding receptors (*1, 3*) (Fig. 1). The delicate equilibrium between the availability of NTs and the survival and maintenance of specific populations of neurons becomes impressively apparent in NT knockout mice (*4–7*). For instance, in mice in which the gene encoding NT-3 has been targeted by homologous recombination, the inactivation of even one allele of the NT-3 gene reduces NT-3 mRNA amounts by about half and results in a massive reduction of cutaneous mechanoreceptors and of the corresponding end organs, the Merkel cells (*8*). Accordingly, in the peripheral sensory and sympathetic nervous systems, specific populations of neurons are supported by specific NTs, and the inactivation of the genes encoding them results in serious characteristic defects of the sensory and sympathetic nervous systems (*4–7*). In contrast, in the central nervous system (CNS) there is much overlap in the trophic support of individual neurons (*9, 10*). The disruption of the expression of an individual factor by gene targeting does not result in changes as dramatic as those in the periphery (*4–7*). Therefore, the results of NT gene targeting experiments in the CNS may, at first sight, appear disappointing, showing at best a reduced expression of choline acetyltransferase (*4*) or of selective neuropeptides and calcium-binding proteins (*6*), which are known to be regulated by different NTs (*6, 9, 11, 12*). However, such gene targeting experiments offer the possibility of identifying subtle NT effects that refine neuronal functions, such as activity-dependent neuronal plasticity. "Neuronal plasticity" is used to describe a great variety of changes in neuronal structure and function, but its use here is confined exclusively to activity-dependent, prolonged functional changes, accompanied by corresponding biochemical and possibly morphological alterations. Indeed, there is increasing evidence that NTs are involved in specific aspects of neuronal plasticity. This evidence originates from observations made in complex integrated systems in vivo, in particular of the influence of prolonged administration of NTs and of corresponding antibodies (Abs) on the development of the rat and cat visual cortex, the most extensively studied and well-understood area of the mammalian cortex (*13*). Although these observations did not reveal the underlying mechanisms, including the identification of individual neurons involved in NT-mediated plasticity, they nevertheless made NTs attractive candidates for the performance of essential roles in the development and activity-dependent modification of neuronal circuits. However, increasingly detailed analyses of the activity-dependent regulation of NT synthesis (*9*), the mechanism and site of NT release from neurons (*14, 15*), and the presynaptic modulation by NTs of the release of classical transmitters (*15–19*) have recently appeared, which are promising with regard to development of a molecular understanding of the more complex integrated systems of established physiological relevance.

Activity-Dependent Regulation of NT Synthesis in the CNS

In contrast to the peripheral nervous system, in the CNS NTs are synthesized predominantly by neurons under physiological conditions (*2, 9*) and, at least in the case of brain-derived neurotrophic factor (BDNF) and NGF, the amounts of these NT mRNAs are regulated by neuronal activity (*9, 20*) in addition to hormonal influences (*9, 11, 21*). Combinations of in vitro and in vivo analyses, performed mostly in the rat hippocampus and cerebral cortex, have demonstrated that the activity-dependent regulation is mediated by classical neurotransmitters. Up-regulation is effected by glutamate via *N*-methyl-D-aspar-

---

The author is in the Department of Neurochemistry, Max Planck Institute for Psychiatry, Am Klopferspitz 18A, D-82152 Martinsried, Germany.